行政法人 國家災害防救科技中心
National Science and Technology Center for Disaster Reduction

Impacts of Polarimetric Radar Data Assimilation on Typhoon Rainfall Nowcasting

Chih-Chien Tsai

2020.10.14

Introduction

NCDR

Outline

- Characteristics of polarimetric radar observations
- Values and limitations of a polarimetric radar observation operator
- Impacts of polarimetric radar data assimilation on typhoon rainfall nowcasting

Case

- Typhoon Soudelor (2015) near landfall in Taiwan
- Assimilation of the RCWF S-band polarimetric radar

Tools

- WRF-LETKF radar assimilation system (Tsai et al. 2014; Yang et al. 2020; Cheng et al. 2020; Wu et al. 2020; You et al. 2020)
- Polarimetric radar observation operator (Jung et al. 2008)

Polarimetric radar

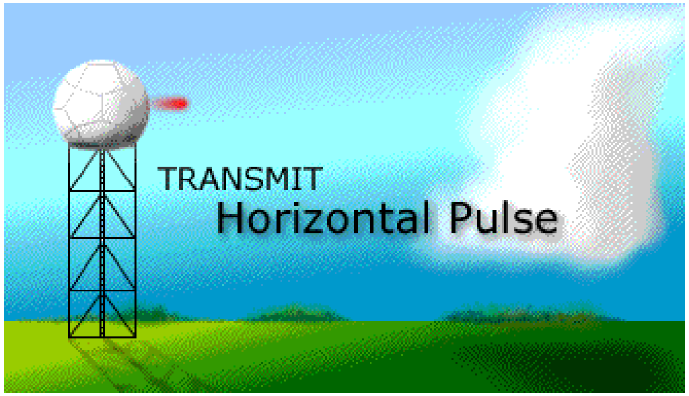

Source: CIMMS

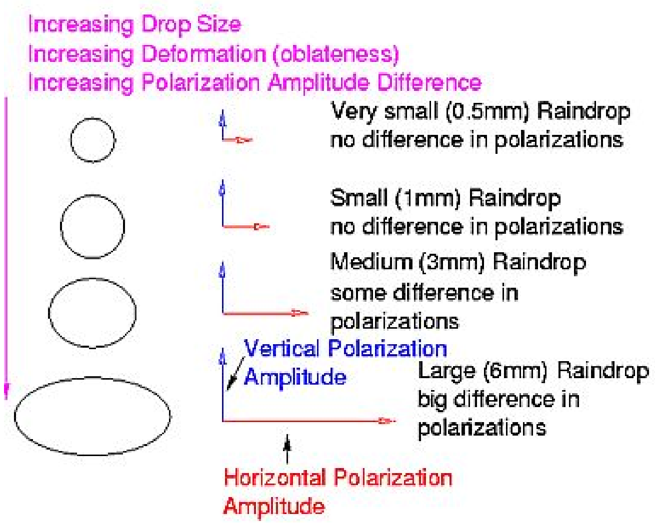

Source: Chilbolton Observatory

Observation variable	Definition
V_R Radial velocity	
Z_H Reflectivity	$Z_H = 10 \log Z_{hh}$
Z_{DR} Differential reflectivity	$Z_{DR} = Z_H - Z_V$
Φ_{DP} Differential phase	$\Phi_{DP} = \Phi_{hh} - \Phi_{vv}$
K_{DP} Specific differential phase	$K_{DP} = \frac{1}{2}\frac{d\Phi_{DP}}{dr}$
ρ_{HV} Copolar correlation coefficient	$\rho_{HV} = \frac{\langle S_{vv} S_{hh}^* \rangle}{\sqrt{\langle \lvert S_{hh} \rvert^2 \rangle \langle \lvert S_{vv} \rvert^2 \rangle}}$

Values

- **Observation-related:**
  - Hydrometeor classification
  - Quantitative precipitation estimation
  - Quality control of radar data
- **Model-related:**
  - Forecast verification
  - Evaluation of cloud microphysics schemes
  - Data assimilation

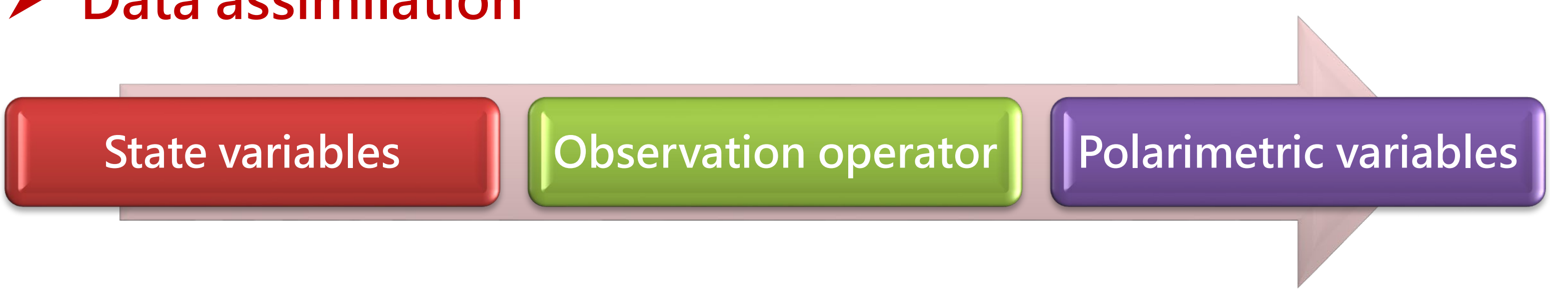

Model configuration

WRF V4.0	
Horizontal grids	280×280 (15 km) 331×331 (3 km)
Eta levels	45 (top at 30 hPa)
Cloud microphysics	**WDM6**
Longwave radiation	RRTM
Shortwave radiation	Goddard
Surface layer	MM5
Land surface model	Noah
Planetary boundary layer	YSU
Cumulus parameterization	Kain-Fritsch
Prognostic state variables	u, v, w, θ', φ', μ', q_v, q_c, q_r, q_i, q_s, q_g, $\boldsymbol{N_{tc}}$, $\boldsymbol{N_{tr}}$, $\boldsymbol{N_{tn}}$

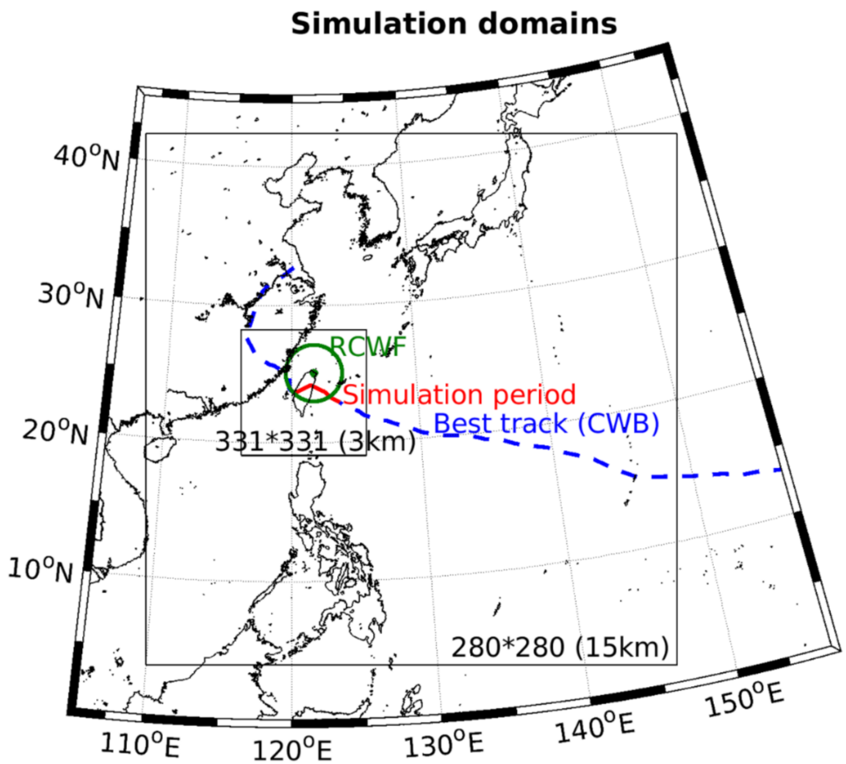

Typhoon Soudelor (2015) near landfall

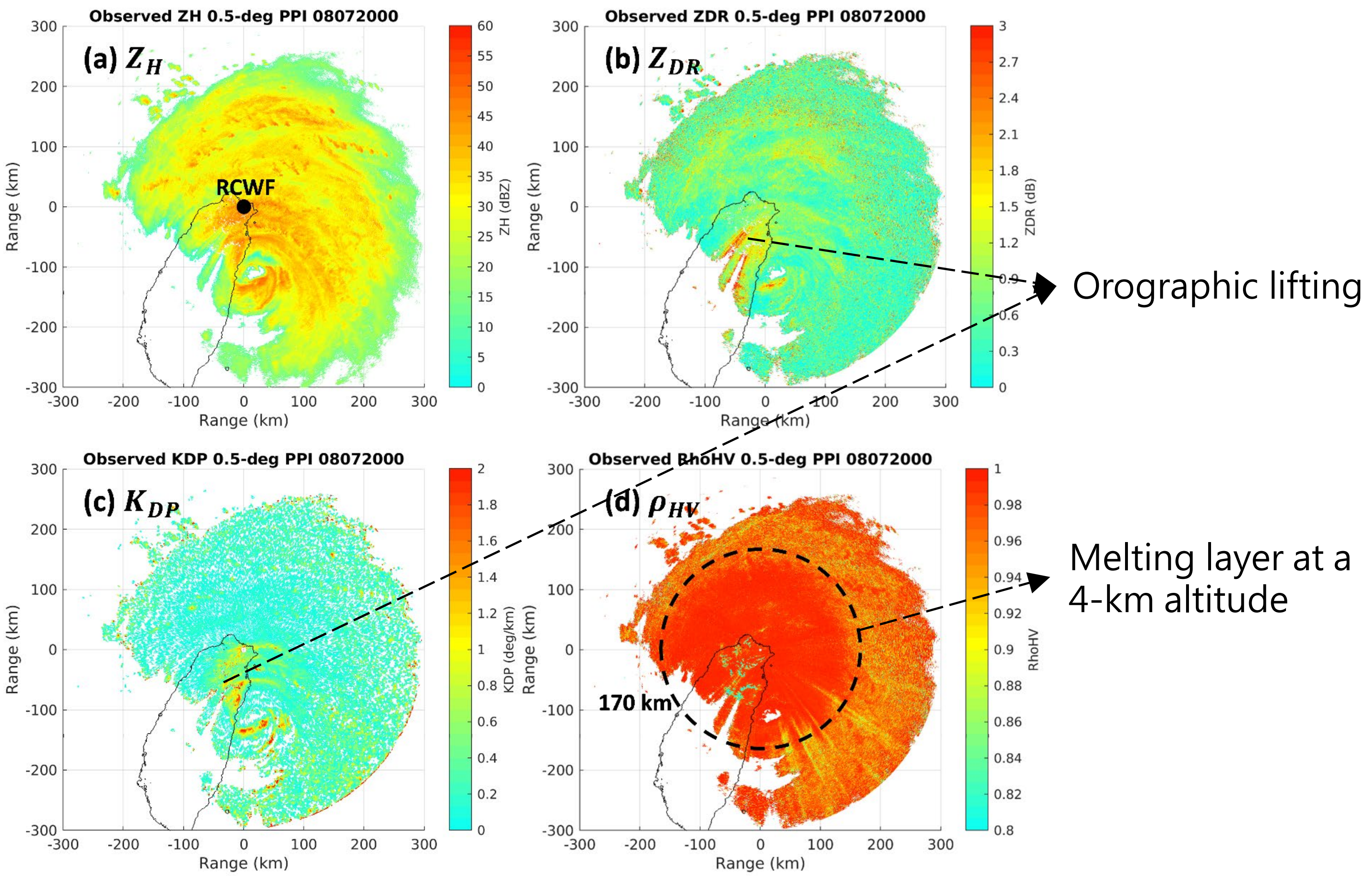

Experimental design

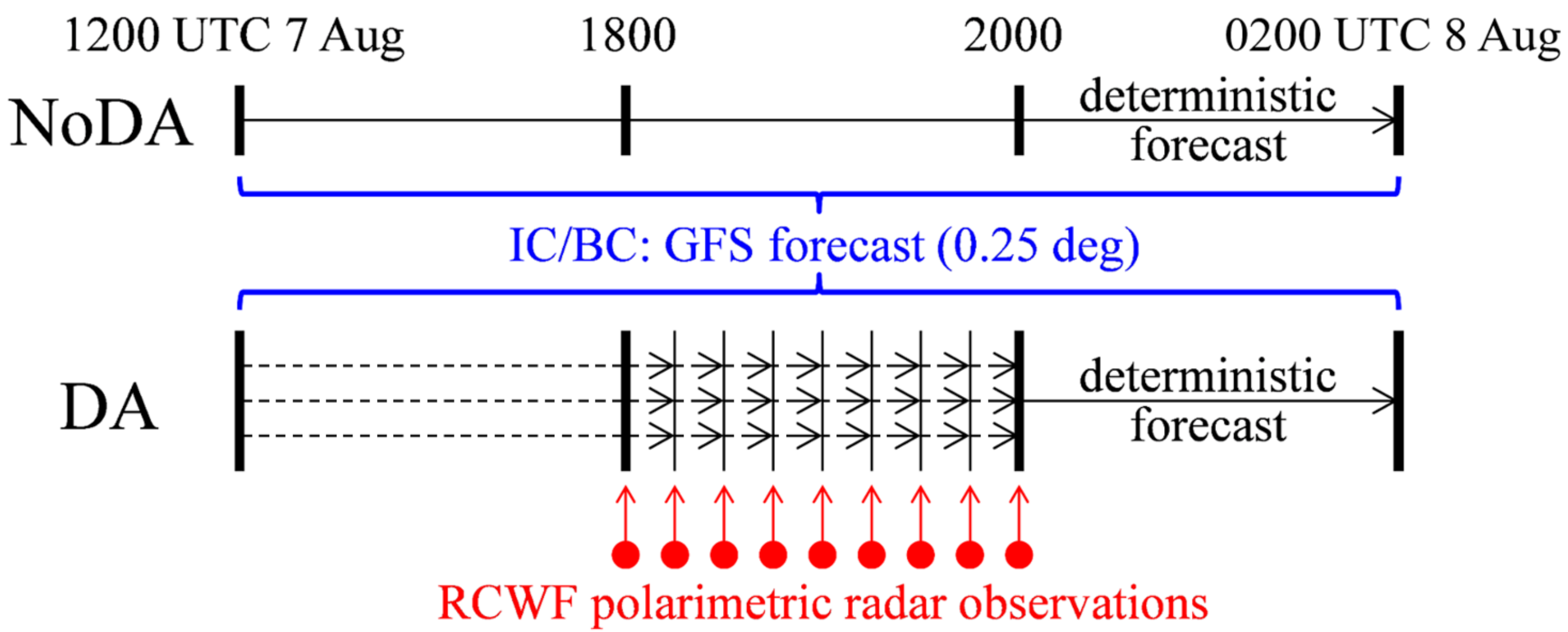

Assessment of the observation operator

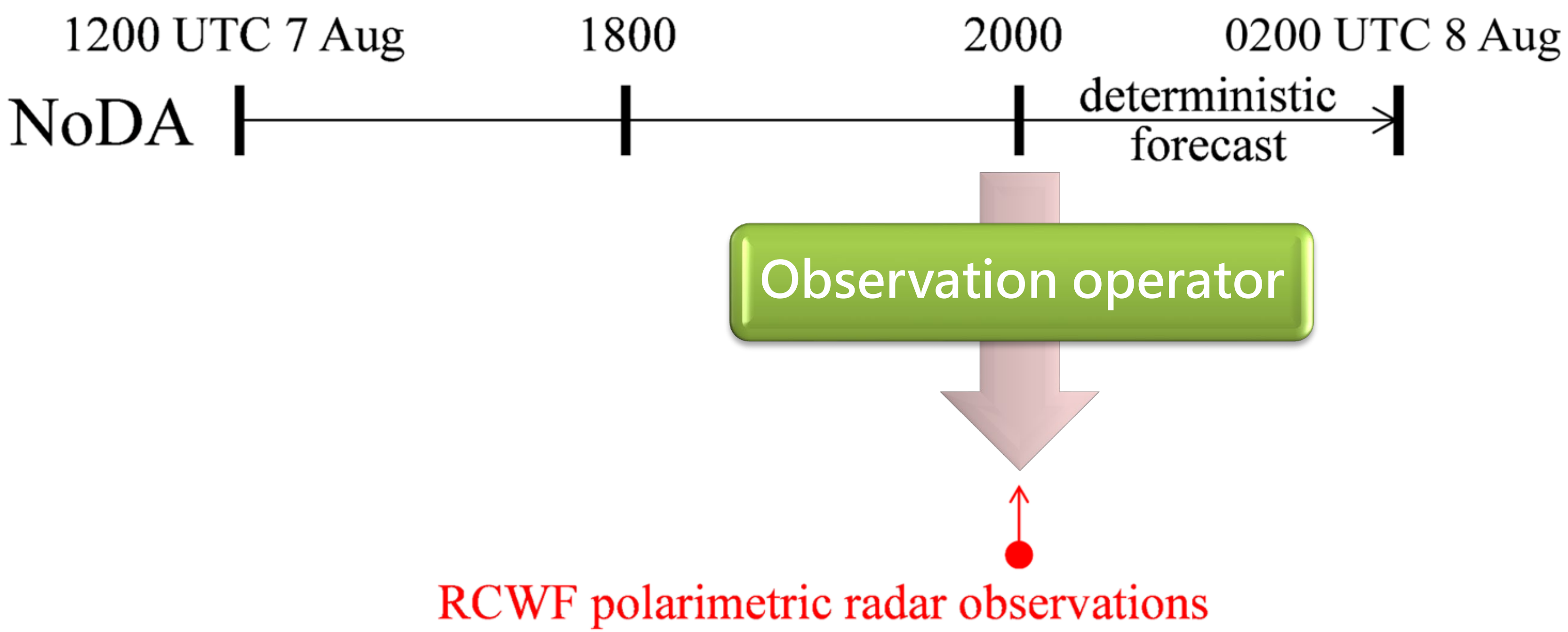

CAPPI at a 3.5-km altitude

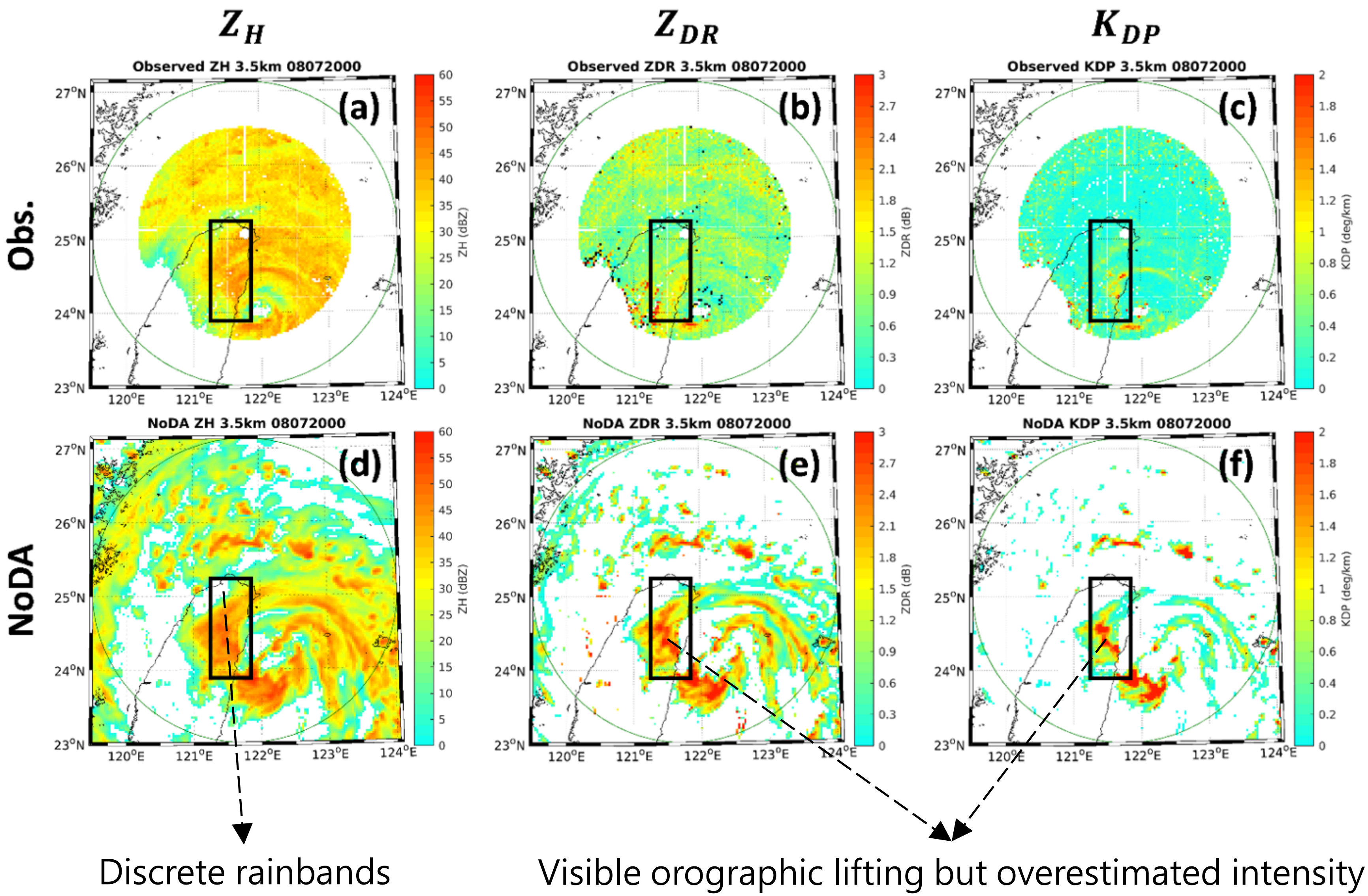

CFAD in convective precipitation areas

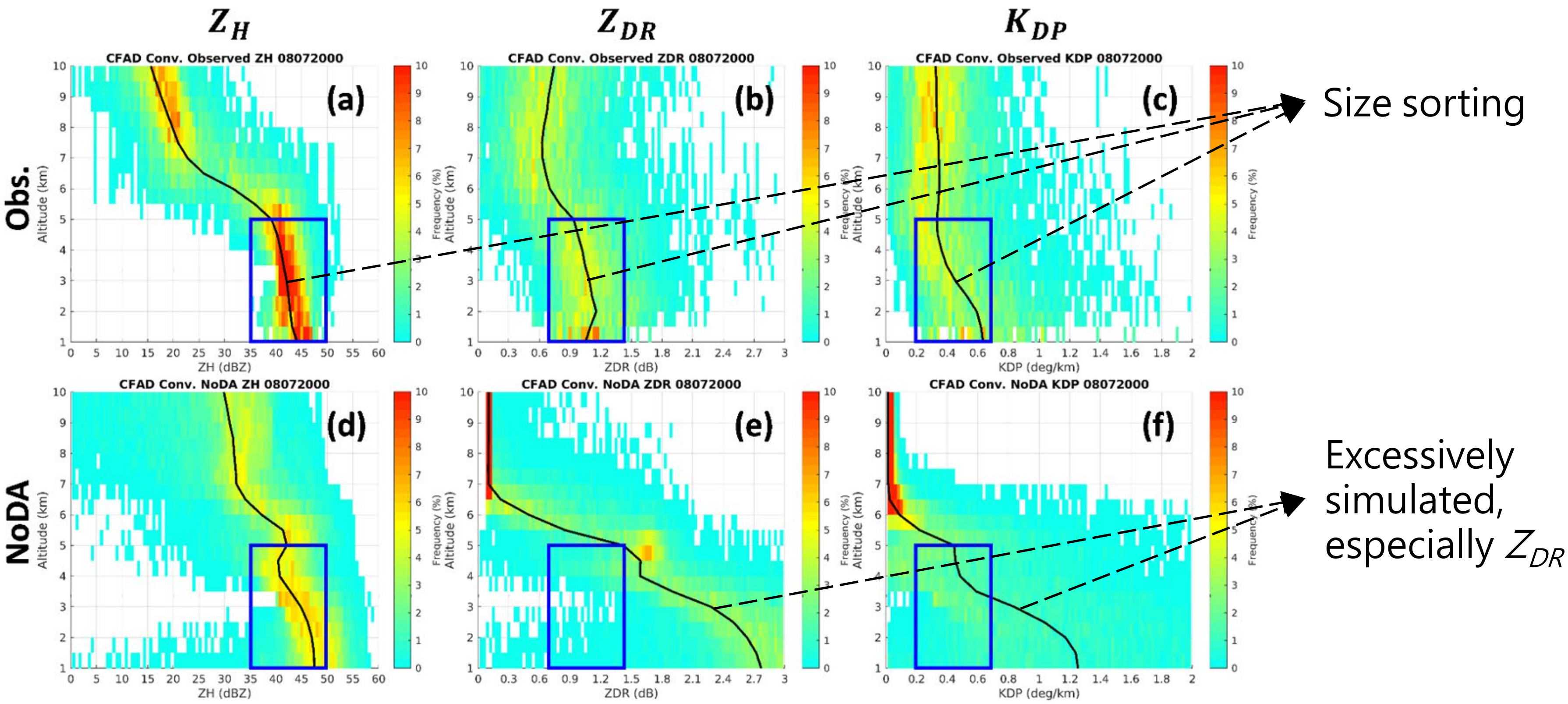

- **Operator error source #1: unsuitable raindrop shape-size relation**
  - Overestimation is maximal for Z_{DR} (most directly related to the raindrop shape) and minimal for Z_H (least)
  - Raindrops tend to be more spherical than theoretical ones in Zhang et al. (2001) according to Chang et al. (2009) observing 13 typhoons that struck Taiwan

CFAD in convective precipitation areas

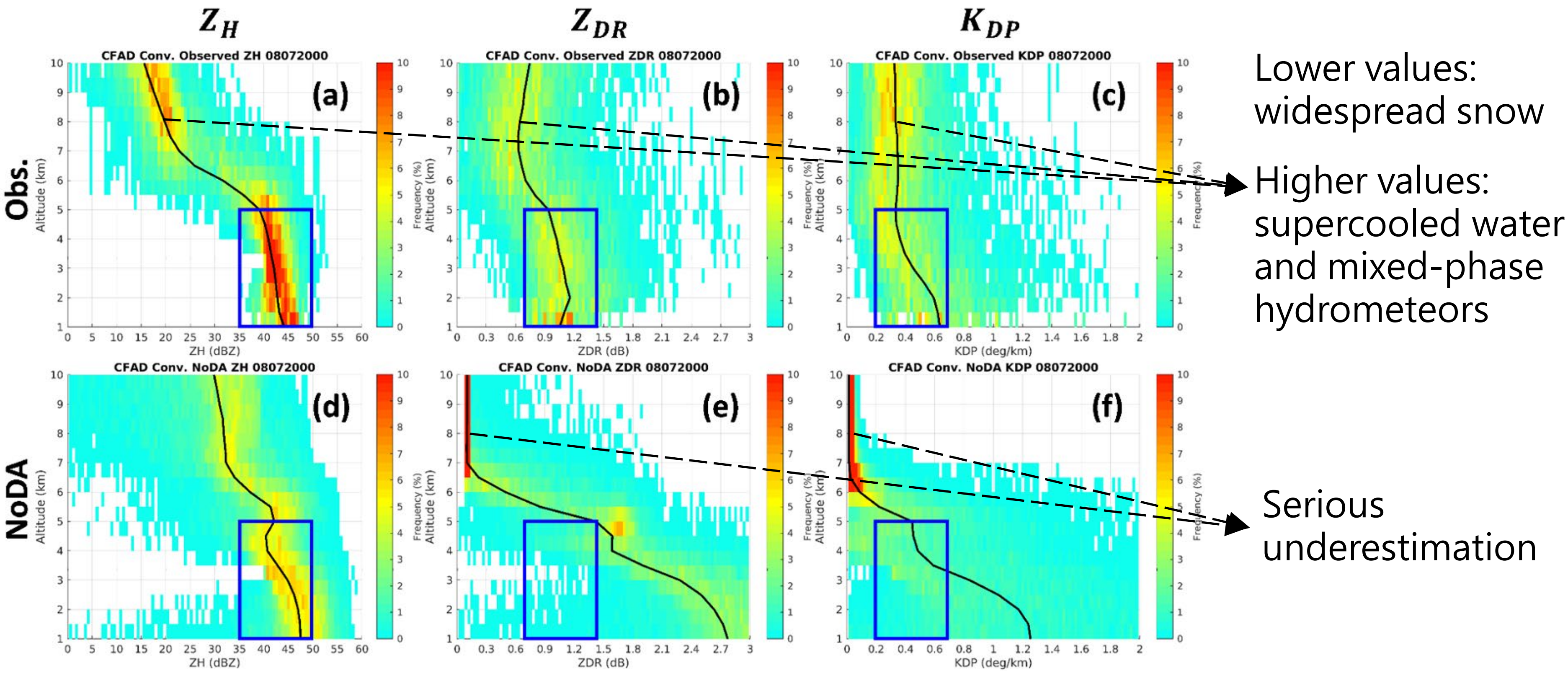

Operator error source #2: limitations for ice-phase hydrometeors

- Snow, graupel, and hail are all treated as ice ellipsoids with the same axis ratio
- Mie scattering may be more realistic for hailstones than Rayleigh scattering
- Ice crystals could be observable when they are vertically aligned by electric fields

CFAD in stratiform precipitation areas

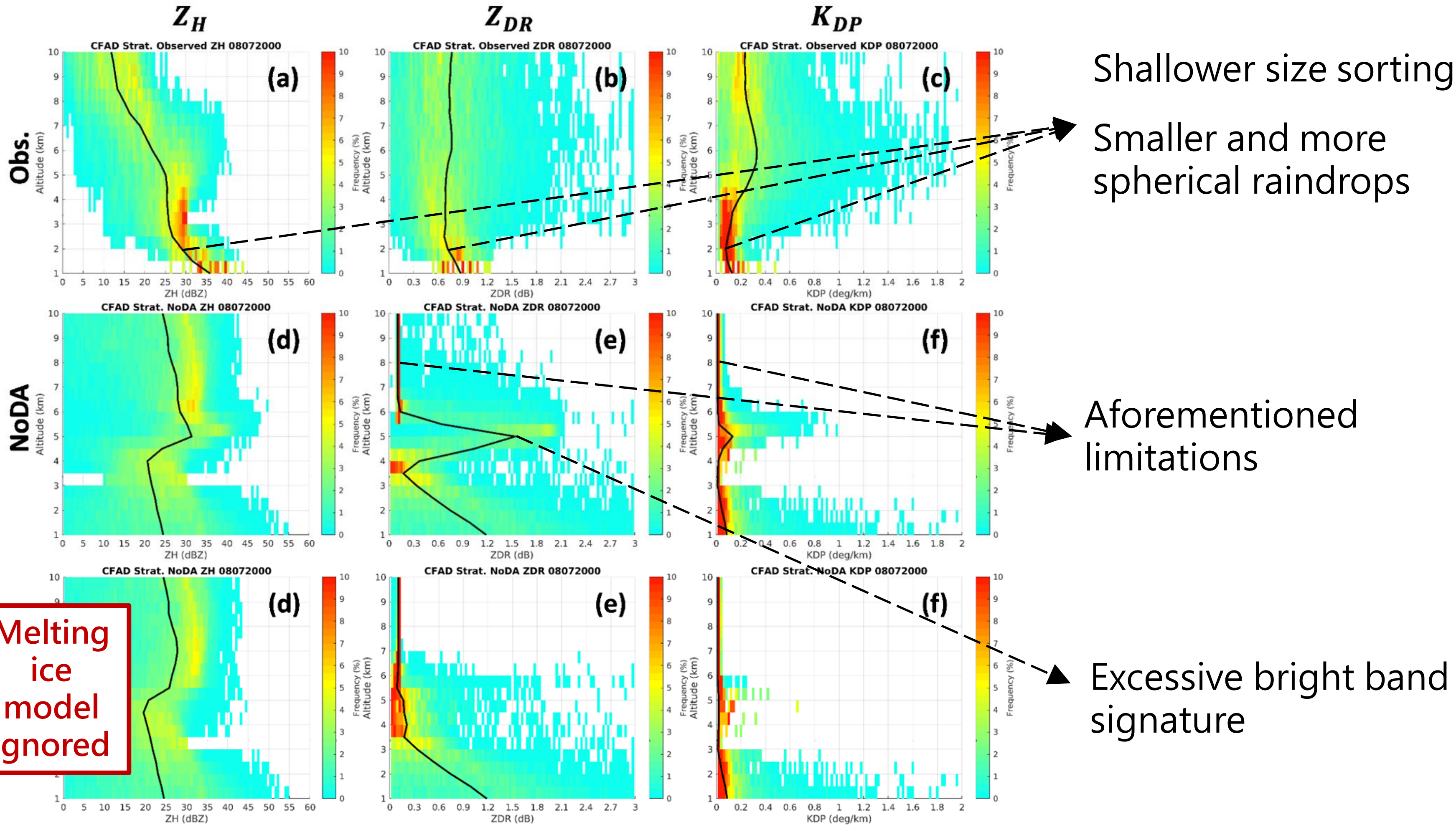

- Operator error source #3: unsuitable melting ice model

Data assimilation experiments

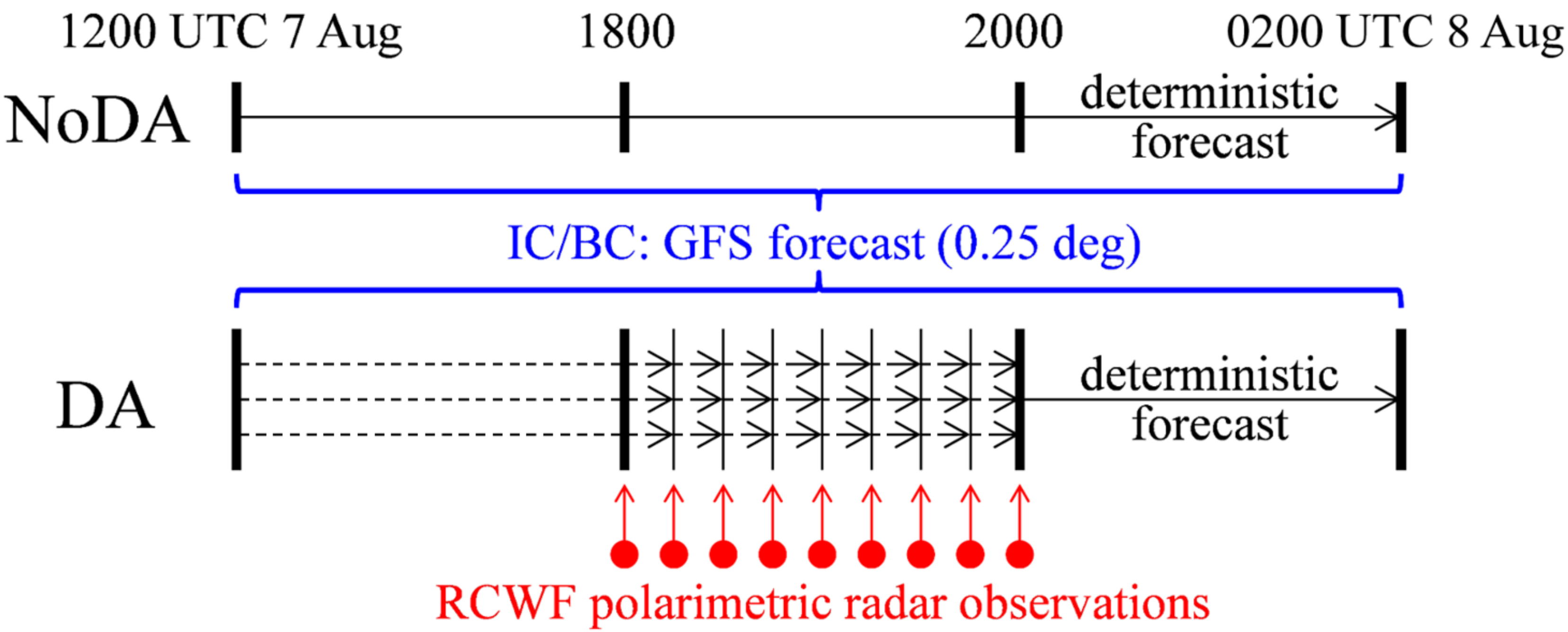

Time (UTC)	Procedure of DA experiments
1200	40-member ensemble perturbed via the random-cv of WRF 3DVar
1200–1800	Spin-up period
1800–2000	Nine LETKF assimilation cycles at a 15-min interval
2000–0200	Deterministic forecast using the analysis ensemble mean

Data assimilation experiments

Name	Assimilatd radar variables
NoDA	None
V	V_r
VZ	$V_r \quad Z_H$
VD	$V_r \quad Z_{DR}$
VK	$V_r \quad K_{DP}$
VZD	$V_r \quad Z_H \quad Z_{DR}$
VZK	$V_r \quad Z_H \quad K_{DP}$
VZDK	$V_r \quad Z_H \quad Z_{DR} \quad K_{DP}$

CAPPI at a 3.5-km altitude

VZ, VD, and VK all correct the discrete rainband pattern

VK slightly mitigates the overestimation of Z_{DR}

VZ and VK, especially the latter, correct the overestimation of K_{DP}

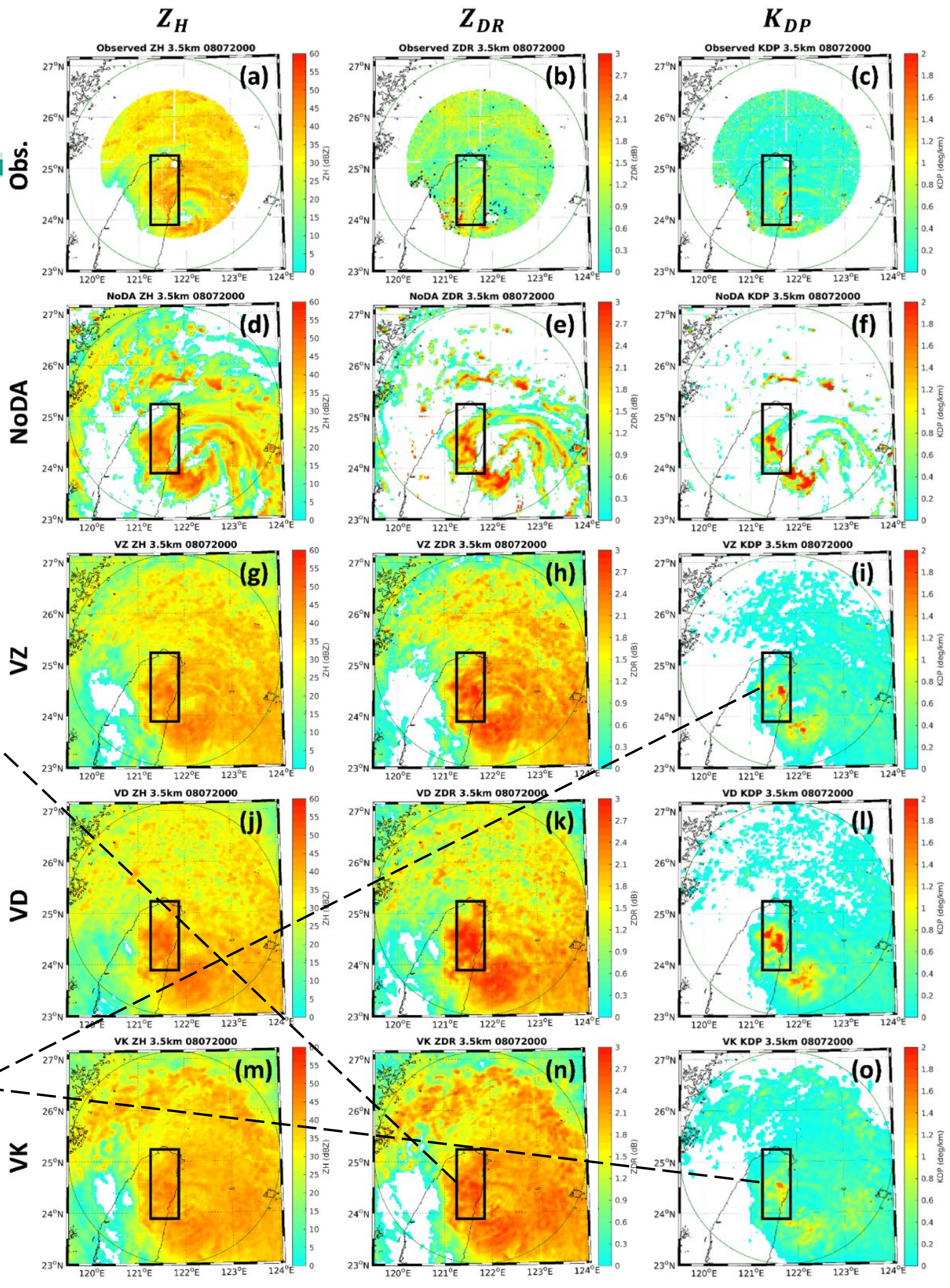

CFAD in convective precipitation areas

VZ, VD, and VK all correct the excessive increasing trend for K_{DP} at lower levels

VK shows the most realistic dispersion for the whole spectra of Z_H and K_{DP}

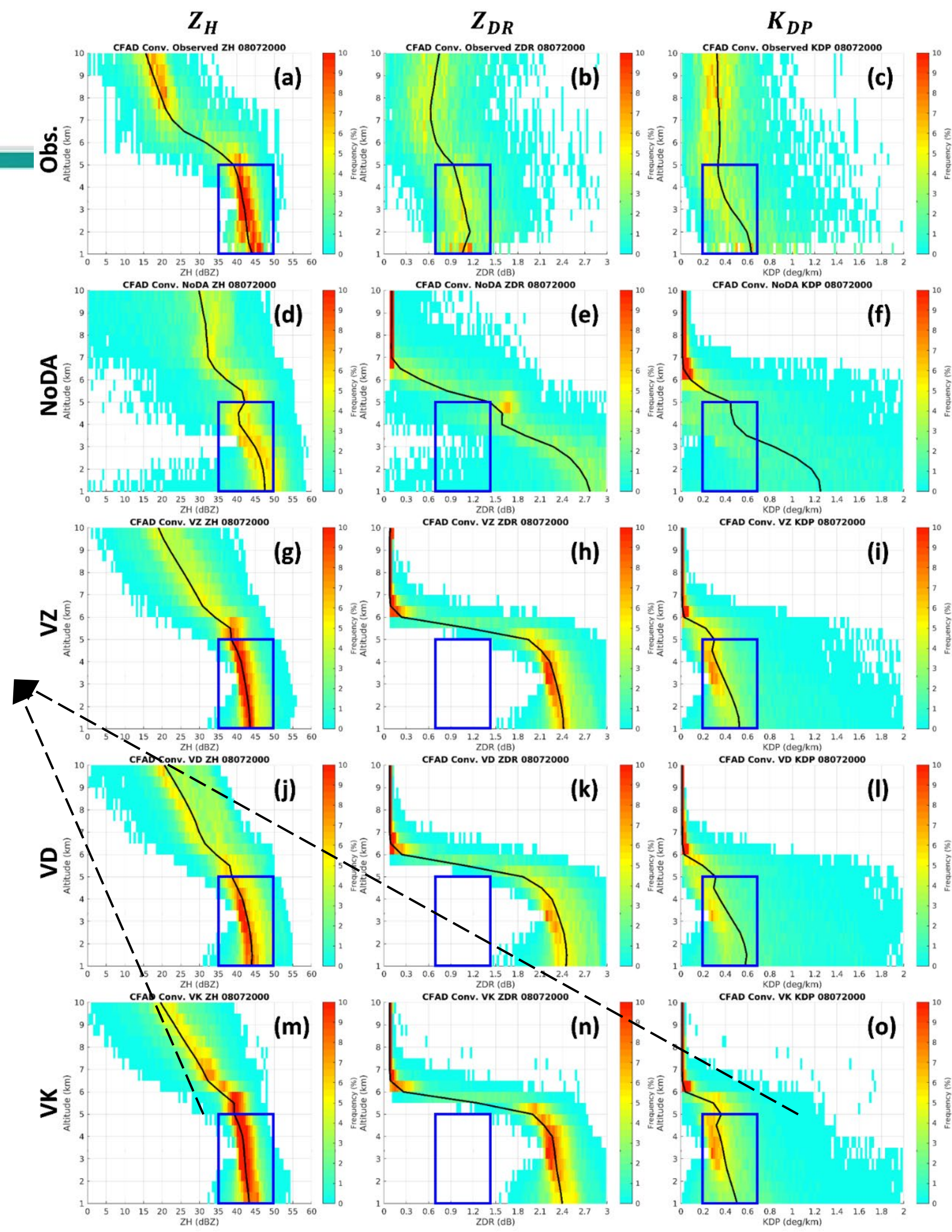

CFAD in stratiform precipitation areas

VZ, VD, and VK all correct the excessive bright band signature for Z_H and Z_{DR}

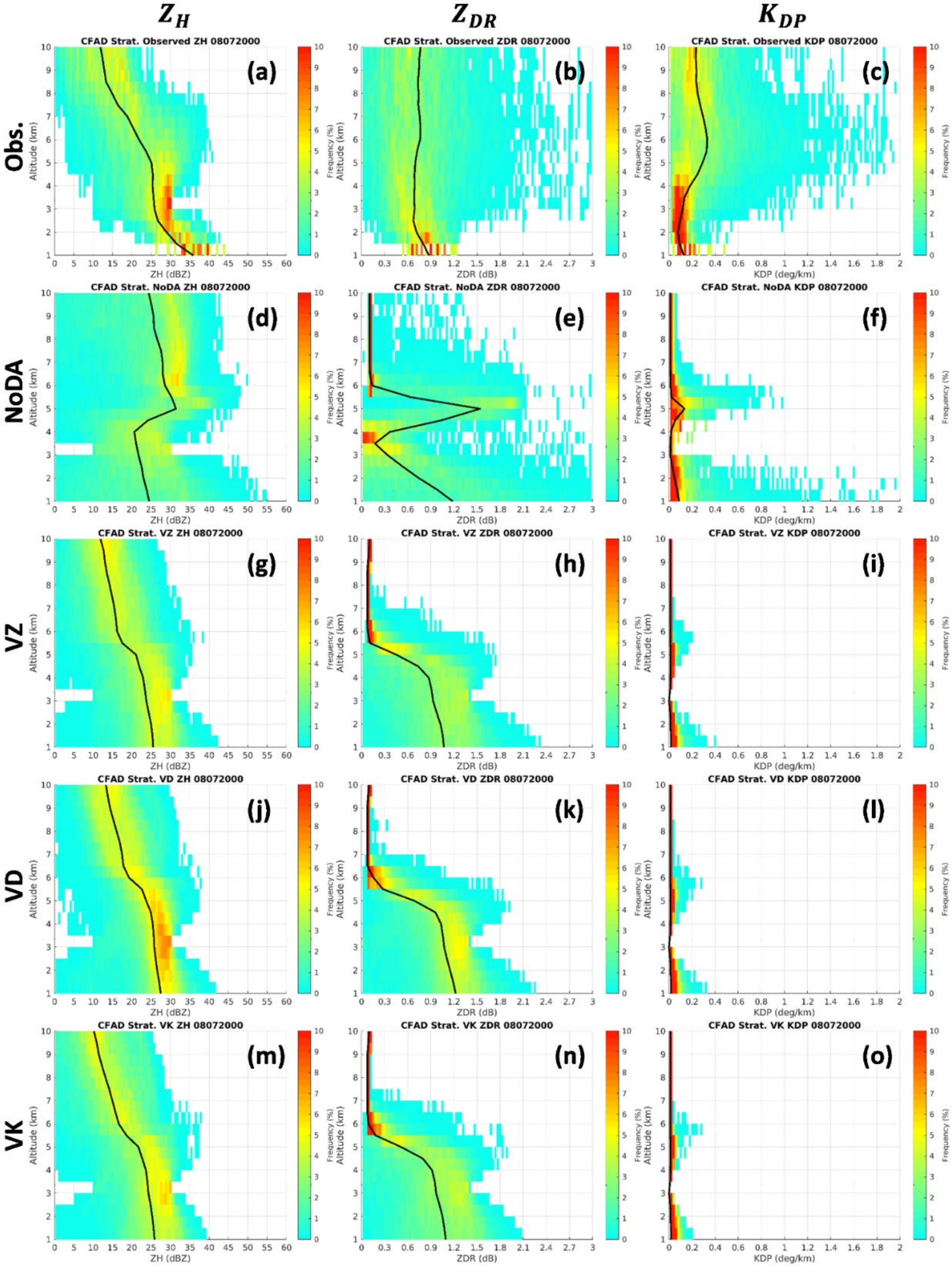

Rainfall nowcasting

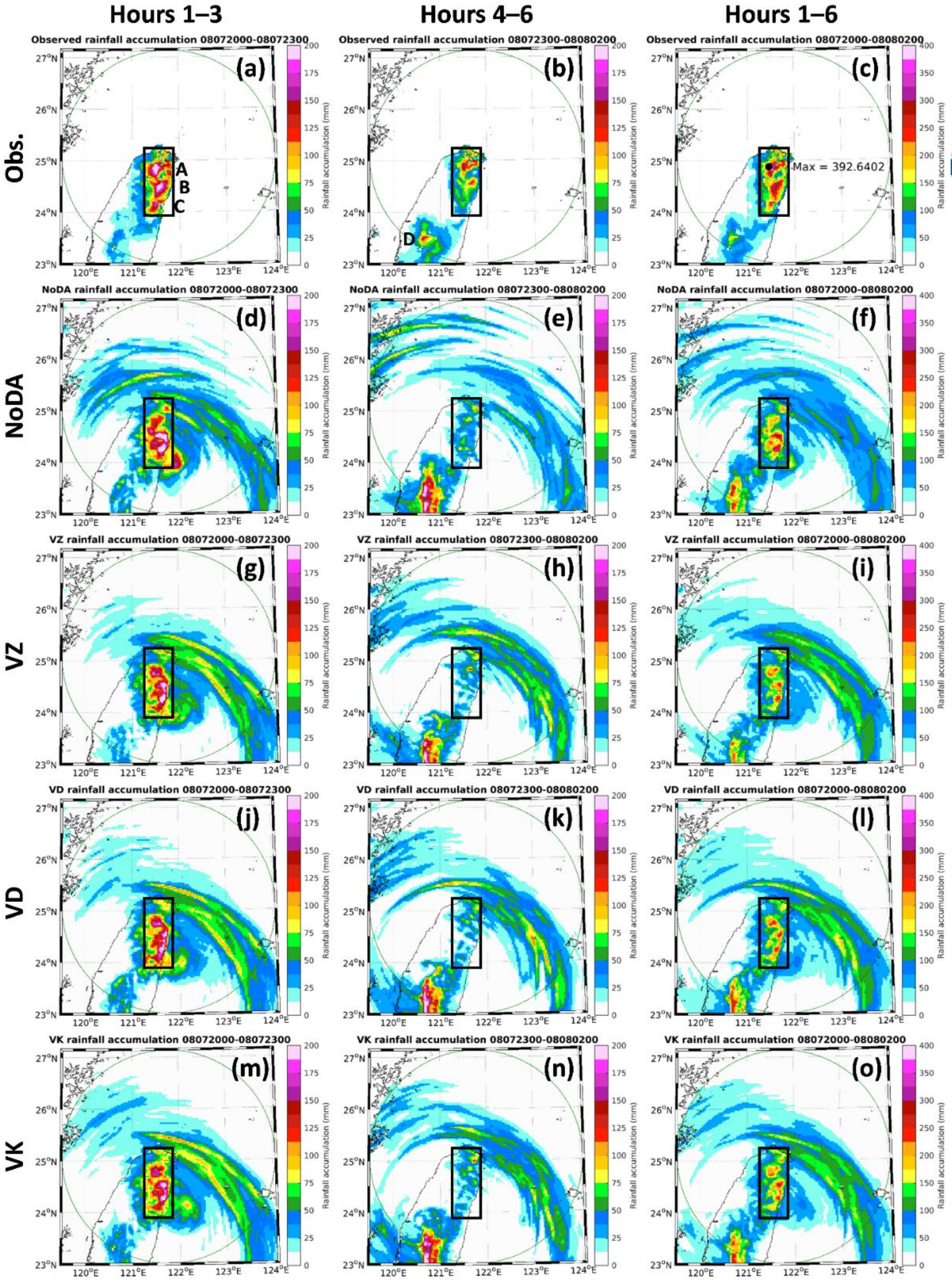

Positive effect of radar data assimilation on predicted rainfall can last 3 hours

Rainfall nowcasting

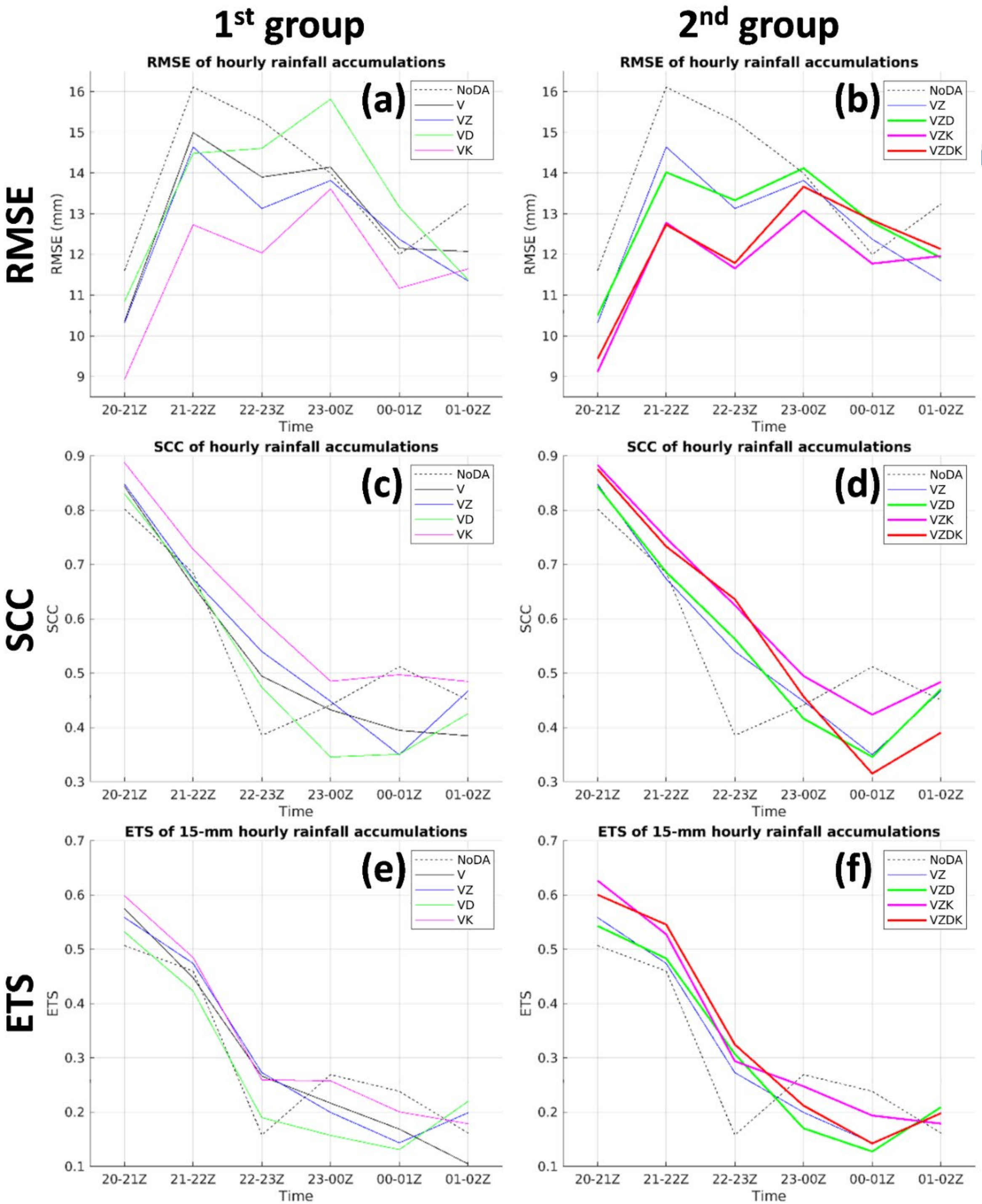

Performance of the 1st group:
VK>VZ>V>VD>NoDA

Performance of the 2nd group:
VZK>VZDK>VZD>VZ>NoDA

Summary

- **Values of the polarimetric radar observation operator:**
  - Forecast verification
  - Evaluation of cloud microphysics schemes
  - Data assimilation
- **Limitations:**
  - Unsuitable raindrop shape-size relation
  - Limitations for ice-phase hydrometeors
  - Unsuitable melting ice model
- **Impacts of polarimetric radar data assimilation:**
  - With the unadjusted observation operator, polarimetric radar data assimilation still corrects the following in observation space:
    1. Discrete rainband pattern
    2. Overestimation of Z_{DR} and K_{DP}
    3. Excessive bright band signature
  - Benefits: $\boldsymbol{K_{DP} > Z_H > Z_{DR}}$
    1. Lower levels of convective precipitation areas
    2. Predicted rainfall
  - Positive effect on predicted rainfall can last **3 hours** by assimilating one S-band polarimetric radar in this typhoon case

References

Chang, W.-Y., T.-C. C. Wang, and P.-L. Lin, 2009: Characteristics of the raindrop size distribution and drop shape relation in typhoon systems in the western Pacific from the 2D video disdrometer and NCU C-Band polarimetric radar. *J. Atmos. Oceanic Technol.*, **26**, 1973–1993.

Cheng, H.-W., S.-C. Yang, Y.-C. Liou, and C.-S. Chen, 2020: An investigation of the sensitivity of predicting a severe rainfall event in northern Taiwan to the upstream condition with a WRF-based radar data assimilation system. *SOLA*, **16**, 97–103.

Jung, Y., G. Zhang, and M. Xue, 2008: Assimilation of simulated polarimetric radar data for a convective storm using the ensemble Kalman filter. Part I: Observation operators for reflectivity and polarimetric variables. *Mon. Wea. Rev.*, **136**, 2228–2245.

Tsai, C.-C., S.-C. Yang, and Y.-C. Liou, 2014: Improving quantitative precipitation nowcasting with a local ensemble transform Kalman filter radar data assimilation system: Observing system simulation experiments. *Tellus A*, **66**, 21804.

Wu, P.-Y., S.-C. Yang, C.-C. Tsai, and H.-W. Cheng, 2020: Convective-scale sampling error and its impact on the ensemble radar data assimilation system: A case study of a heavy rainfall event on 16 June 2008 in Taiwan. *Mon. Wea. Rev.*, **148**, 3631–3652.

Yang, S.-C., Z.-M. Huang, C.-Y. Huang, C.-C. Tsai, and T.-K. Yeh, 2020: A case study on the impact of ensemble data assimilation with GNSS-zenith total delay and radar data on heavy rainfall prediction. *Mon. Wea. Rev.*, **148**, 1075–1098.

You, C.-R., K.-S. Chung, and C.-C. Tsai, 2020: Evaluating the performance of a convection-permitting model by using dual-polarimetric radar parameters: Case study of SoWMEX-IOP8. *Remote Sens.*, **12**, 3004.

Zhang, G., J. Vivekanandan, and E. Brandes, 2001: A method for estimating rain rate and drop size distribution from polarimetric radar measurements. *IEEE Trans. Geosci. Remote Sens.*, **39**, 830–841.